FEBS Letters 581 (2007) 3517–3522

An apoptosis-related gene network induced by novel compound-cRGD in human breast cancer cells

Tsui-Chin Huang[a], Hsuan-Cheng Huang[b], Chih-Chin Chang[b], Hsin-Yi Chang[a], Chern-Han Ou[c,d], Chun-Hua Hsu[e], Shui-Tein Chen[f,g], Hsueh-Fen Juan[a,c,*]

[a] *Institute of Molecular and Cellular Biology, National Taiwan University, Taipei, Taiwan*
[b] *Institute of Bioinformatics, National Yang-Ming University, Taipei, Taiwan*
[c] *Department of Life Science, National Taiwan University, Taipei,Taiwan*
[d] *Department of Electronic Engineering, National Taiwan University, Taipei, Taiwan*
[e] *Institute of Molecular Biology, National Chung-Hsing University, Taichung, Taiwan*
[f] *Institute of Biological Chemistry and the Genomics Research Center, Academia Sinica, Taipei, Taiwan*
[g] *Institute of Biochemical Sciences, National Taiwan University, Taipei, Taiwan*

Received 24 February 2007; revised 25 June 2007; accepted 26 June 2007

Available online 3 July 2007

Edited by Varda Rotter

Abstract **Synthetic peptides with the arginine-glycine-aspartate (RGD) motif have been used widely as inhibitors of integrin–ligand interactions to study cell growth, adhesion, migration and differentiation. We designed cyclic-RGD peptide (Tpa-RGDWPC-, cRGD) which could cause cell death in MCF-7 cell line. In order to understand the mechanism involved in cRGD-induced apoptosis, we used microarray, real-time quantitative PCR (Q-PCR) and bioinformatics to study the effects of cRGD on breast cancer cell line MCF-7. By time-series gene expression measurements and our developed software BSIP and GeneNetwork, we reconstructed an apoptosis-related gene network. In the network, caspase-9, located at the upstream, activates downstream effector caspases such as caspase-7, leading to the induction of caspase-4. Combined our previous proteomics data with newly performed docking simulation, it indicated that the cell death induced by cRGD may be triggered through blocking integrin signaling to the extracellular matrix and activation of caspase pathway. This study provides a molecular explanation of cRGD treatment in breast cancer cells and set forth a constructive far-reaching impact on breast cancer therapy.**

Keywords: Apoptosis; cRGD; Integrin; MCF-7; Caspase

1. Introduction

Apoptosis is a programmed cell death involved in many physiological and pathological regulations [1]. Defective regulation of apoptosis leads to a variety of human diseases including cancer, autoimmune diseases and neurodegenerative disorders [2]. Currently, understanding of apoptosis mechanisms has resulted in new strategies for treating certain illnesses, and several clinical testing are undergoing. Apoptosis is typically accompanied by the activation of a class of death proteases called caspases. The apoptotic pathway is consisted of several triggers, modulators and effectors. Loss of adhesion of integrins to their ligands is one such trigger. Integrins are heterodimeric cell surface receptors that mediate cell–cell and cell–extracellular matrix (ECM) interactions. Functions of integrins have been shown to be involved in several important cellular processes, including cell differentiation, angiogenesis, apoptosis, cell migration, and tumor growth [3].

Synthetic peptides with the arginine-glycine-aspartate (RGD) motif have been used widely as inhibitors of integrin–ligand interactions in studies of cell adhesion, migration, growth, and differentiation [4,5]. Recently, RGD peptides have also been found to induce apoptosis in cells such as MDCK cells [6], glomerular mesangial cells [7], and lymphocytes [8]. Former evidence shows that RGD-containing peptide may induce an anchorage-independent apoptosis of HL60 cells and T cells by entering into the cell and directly promoting caspase-3 activation [5,9,10]. Buckley et al. showed that the breast carcinoma cell line MCF-7 with a functional deletion of the caspase-3 gene was not inhibited in cell growth after RGD peptides treatment [5]. However, our previous report [11] shows MCF-7 suffered apoptosis after the treatment of our designed cyclic Tpa-RGDWPC (cRGD). This gives rise to the question, how cRGD inhibits cell growth of MCF-7 cells by apoptotic pathway. We used a systems biology approach combining with microarray, real-time quantitative PCR (Q-PCR) and bioinformatics techniques to understand the molecular mechanism of the cRGD induced apoptosis in MCF-7 cells. With time-series gene expression measurements and our developed software, GeneNetwork and BSIP, an apoptosis-related gene network has been reconstructed.

2. Materials and methods

2.1. Synthesis of cyclic RGD

Cyclic RGD peptide (cyclic-3-mercaptopropionic acid-Arg-Gly-Asp-Trp-Pro-Cys) (Fig. 1) was synthesized by solid-phase Fmoc chemistry using Rink amide resin. The crude peptide was purified by RP-HPLC C18 preparative column (10 mm × 250 mm); H_2O containing 0.1% TFA/acetonitrile containing 0.1% TFA from 95/5 to 5/95 in 30 min with a flow rate of 4 ml/min. The purity (>90%) was determined by analytical C18 HPLC and mass spectrometry.

*Corresponding author. Address: Department of Life Science, National Taiwan University, No. 1, Sec. 4, Roosevelt Road, Taipei, 106 Taiwan. Fax: +886 2 23673374.
E-mail address: yukijuan@ntu.edu.tw (H.-F. Juan).

Abbreviations: Tpa-RGDWPC, cRGD; Q-PCR, quantitative PCR

0014-5793/$32.00
doi:10.1016/j.febslet.2007.06.067

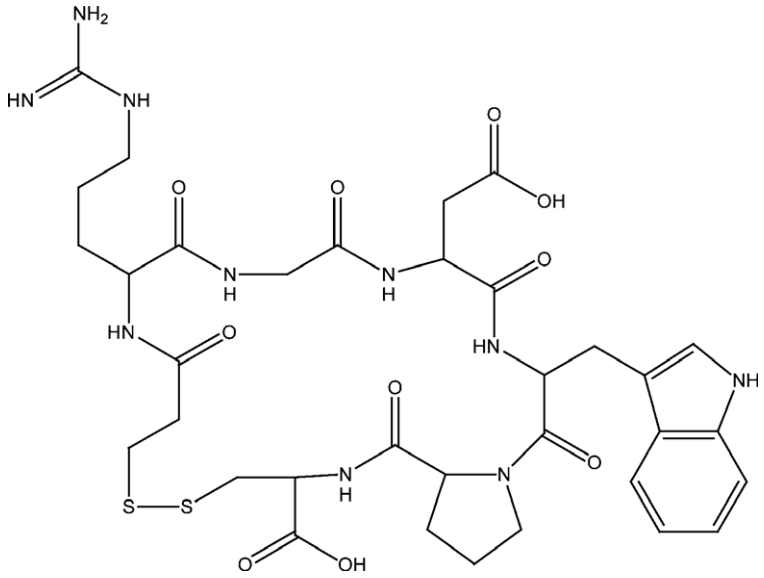

Fig. 1. The structure of cRGD.

2.2. Docking of cRGD with integrin

In order to further understand the interaction of RGD with integrin, a docking experiment was performed using the receptor molecular model and docking protocol as described previously [12]. This protocol, using the shape-based docking algorithm LigandFit [13], consists of the flexible fitting of the ligand (cRGD) within a rigid receptor (integrin- PDB entry 1L5G). The obtained poses were subsequently scored using the scoring function, LigScore [14]. The best pose was then energy minimized with CHARMm [15], allowing full flexibility for the ligand and only side-chain flexibility for the receptor. All calculations were carried out in the Discovery Studio 1.6 environment (Accelrys, San Diego, CA).

2.3. Cell culture

Human breast cancer MCF-7 cells were maintained in Dulbecco's modified Eagle's medium (Atlanta Biologicals, GA, USA) supplemented with 10% fetal bovine serum (Gibco BRL, NY, USA), 1.5 g/l sodium bicarbonate (Atlanta Biologicals), 4.5 g/l glucose, 4 mM L-glutamine, 1 mM sodium pyruvate, penicillin (100 U/ml), streptomycin (100 μg/ml), and amphotericin B (0.25 μg/ml, Atlanta Biologicals). Cells were cultured at 37 °C in an incubator with humidified atmosphere of 5% CO_2 in air.

2.4. RNA extraction

Total RNA was extracted from cyclic-RGD-treated (1 mM) and non-treated MCF-7 cells. Briefly, the cultured cells were harvested and lysed with Trizol reagent (Invitrogen, Carlsbad, CA) following the manufacturer's instructions. The purified RNA was quantified by a UV spectrophotometer, and RNA quality was evaluated by capillary electrophoresis on an Agilent 2100 Bioanalyzer (Agilent Technologies, Palo Alto, CA).

2.5. Time-course cDNA microarray

The data, both control and treated set, were obtained after cRGD treatment at 6, 24, 48, 72 h to show the kinetics profile of gene expression. Total RNA was reverse transcribed using the Agilent direct-label cDNA synthesis kit (Agilent Technologies) and following the manufacturer's directions. Labeled cDNA was purified using QIAquick PCR Purification columns (Qiagen, Valencia, CA). In this study, RNA from cRGD treated MCF-7 cell was labeled with Cyanine 5-dCTP, and untreated one was labeled with Cyanine 3-dCTP. The combined Cy3- and Cy5-labeled cDNAs were hybridized to an Agilent Human 1 cDNA microarray according to the manufacturer's protocol (Agilent Technologies). Subsequently, the arrays were scanned using a dual-laser Microarray Scanner G2565AA (Agilent Technologies). Normalization for each gene and comparative analysis between expression profiles was carried out using GeneSpring version 7.3 (Silicon Genetics, Redwood, CA).

2.6. Real-time Q-PCR

Total RNA was reverse-transcribed into cDNA by using an oligo(dT)20 primer and SuperScript III Reverse Transcriptase (Invitrogen). The specific gene primers for real-time PCR were designed using the Beacon Designer 2.1 program (Premier Biosoft International, Palo Alto, CA). Sequences are shown in Table 1. The real-time PCR reaction (25 μl) containing 5 μl first-strand cDNA, 12.5 μl iQ SYBR Green supermix kit (Bio-Rad Laboratories, Hercules, CA) and 0.5 μl (10 μM) of each sense and antisense primer was run for 40 amplification cycles in an iCycler iQ Real-Time PCR Detection System (Bio-Rad Laboratories). Cycling conditions were 95 °C for 3 min, 95 °C for 30 s, and 60 °C for 30 s. Relative transcript quantities were calculated using the $\Delta\Delta C_t$ method with β-actin as the reference gene amplified from the samples. All reactions were run in triplicate.

Table 1
Primers used for real-time PCR analysis

	Sense primer	Anti-sense primer	Accession number
Caspase 1	ACACCGCCCAGAGCACAAG	CTTCCCACAAATGCCTTCCCG	NM_001223
Caspase 2	TGGGTGCGAGGAGAGTGATG	TGGCGGCAGTCCCTTTGAG	NM_001224
Caspase 4	TCACCTGCCTGCAAGGAATG	TGGCGTTGAAGAGCAGAAAGC	NM_001225
Caspase 5	CTGGAGAGACCGCACAAGGG	TCGTCAACCACAGTGTAGCC	NM_004347
Caspase 6	GCCACGCAGATGCCGATTG	CCAACCAGGCTGTGACACTTG	NM_001226
Caspase 7	GTCTCACCTATCCTGCCCTCAC	TTCTTCTCCTGCCTCACTGTCC	NM_001227
Caspase 8	GAAAAGCAAACCTCGGGGATAC	CCAAGTGTGTTCCATTCCTGTC	NM_001228
Caspase 9	CCAGAGATTCGCAAACCAGAGG	GAGCACCGACATCACCAAATCC	NM_001229
Caspase 10	AGCCGAGTCGTATCAAGGAGAG	GCCTCTGTGGTTCCGATTCATC	NM_032976

All primers are listed 5′–3′.

2.7. Significance analysis of Q-PCR experiments

Significance analysis of Q-PCR experiments was performed by EDGE [16] which is a software tool based on optimal discovery procedure and time course methodology for the significance analysis of time-course experiments.

2.8. Network construction

Based on the time-course Q-PCR data, we used our developed software BSIP and GenNetwork [17] to construct the plausible gene regulatory network of cRGD-induced apoptosis in MCF-7 cells.

2.9. Western blotting

The proteins are extracted using lysis buffer containing 7 M urea (Boehringer, Mannheim, Germany), 2 M thiourea, 4% CHAPS (J.T. Baker, Phillipsburg, NJ, USA) and 0.002% bromophenol blue (Amersco, OH, USA). After electrophoresis, proteins were blotted onto polyvinyl-difluoride membranes (MILLIPORE, MA, USA). After blocking in 5% nonfat milk in PBST containing 0.1% Tween 20 (J.T. Baker) at room temperature 1 h with gentle shaking, membranes were probed with antibodies. Primary antibodies involved in this study include caspase-9 (Clone 96-2-22, Upstate, NY, USA) and caspase-7 (Cell Signaling Technology, Inc., MA, USA) both diluted in 1:1000. Membranes were incubated with corresponding primary antibody and then incubated with secondary antibodies (anti-mouse IgG-HRP, 1:5000 dilution, Abcam, Cambridge, UK). After incubation with secondary antibodies, immunoblots were visualized with the ECL detection kit (Pierce Biotechnology Inc., IL, USA) and exposed to Fuji medical X-ray film. β-Actin was used as an internal loading control.

3. Results

3.1. Protein–ligand interaction estimated by docking simulation

In order to further understand the interaction of RGD with integrin, the docking experiments were performed on the Discovery Studio 1.6 environment. The output convergent conformations demonstrated that our designed cRGD has a reliable binding affinity to integrin interface. The predicted integrin–cRGD complex conformation was illustrated in Fig. 2A. The RGD sequence makes the main contact area with the integrin, and each residue participates extensively in the interaction. The RGD residues which formed hydrogen bonds with integrin β subunit interacted with Asp127, Asn313, and Arg248 residues (Fig. 2B).

3.2. Gene expression profiles induced by cRGD in MCF-7

To identify genes involved mainly in apoptosis, and to compare the difference of gene expression in treated cells and untreated ones, we utilized a complimentary DNA microarray

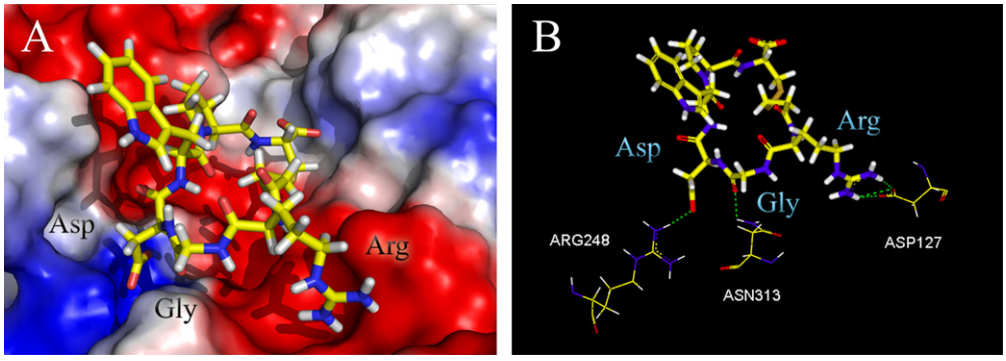

Fig. 2. Binding mode of cRGD with integrin (PDB code: 1L5G). (A) cRGD is docked in the integrin active site. Hydrophobic (white), negatively-charged (red), and positively-charged (blue) surfaces. The picture is prepared with PyMol [23]. (B) The cRGD molecule is formed hydrogen bond with integrin by RGD residue. The picture is prepared with Discovery Studio 1.6 environment.

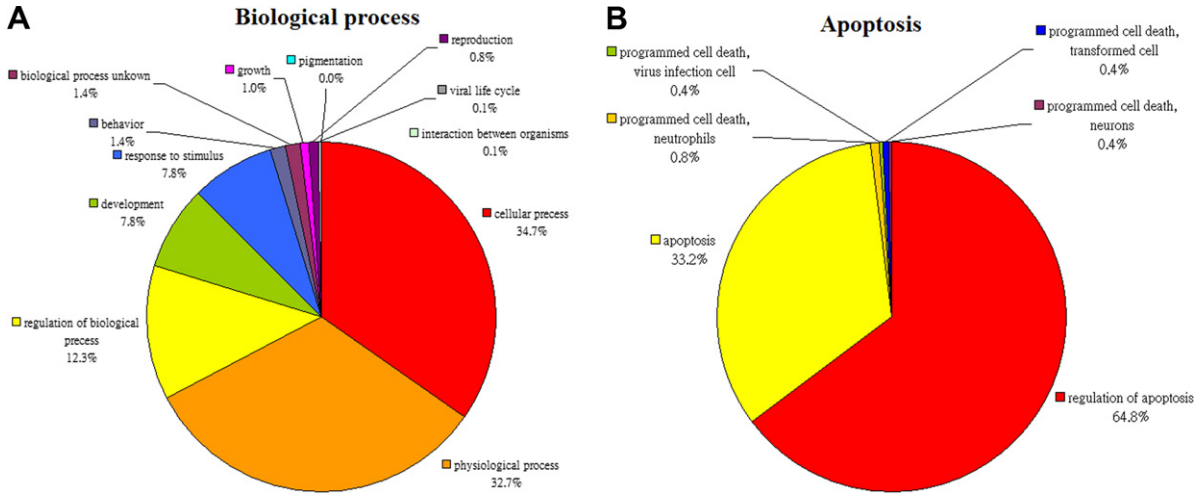

Fig. 3. A pie chart representing the distribution of functional classifications of cRGD-treated human breast carcinoma cell line MCF-7 based on the Gene Ontology assignments generated by GeneSpring software. (A) Genes that were expressed at each stage after treatment, and clustered by biological process showed in percentages. (B) 253 of these genes which are related to apoptosis.

Table 2
Fold change of caspase gene expression

Description	Genebank accession no.	6-h-fold change	24-h-fold change	48-h-fold change	72-h-fold change
Caspase 4, apoptosis-related cysteine protease	U28976	1.198754	1.389036	1.52571	2.511147
Caspase 6, apoptosis-related cysteine protease	U20536	0.928076	0.948146	0.965973	0.464663
Caspase 7, apoptosis-related cysteine protease	U67319	1.175194	1.201633	1.115639	1.391235
Caspase 9, apoptosis-related cysteine protease	U60521	1.005501	1.091598	1.628327	1.171525

carrying approximately 13000 human genes. Transcription profiles were monitored 6, 24, 48 and 72 h after the onset of treatment. From the analysis of cDNA microarray data, genes shown in Fig. 3 were found to be either 2-fold up- or down-regulated in at least one of four time points compared with control samples. For an overall functional interpretation of the common responses, these genes were sorted into groups according to their gene ontology (GO) database categories for biological processes (GO: http://www.geneontology.org). This database provides annotations regarding the functions and signaling of each gene. Pie charts were then constructed to present the data. These genes which were categorized into classes based on GO were represented in percentage (Fig. 3A). cRGD regulates the expression of genes associated with a broad range of biological process. The largest group of genes is associated with "cellular process", while "physiological process" and "regulation of biological process" are the next most abundant groups of gene annotations. There are 253 genes related to apoptosis (Fig. 3B). The genes have been generated with specific importance in "regulation of apoptosis", "apoptosis", and "programmed cell death". Several apoptosis-related genes such as caspase genes, bcl2, TNF receptor-associated factor 3, interleukin 1β, and protein kinase C ε represented differential expressions in the microarray profile (data not shown). Among them, the caspase genes we are interested in were shown in Table 2. Accordingly, we focused on the major caspase family genes, listed from caspase-1 to −10, and verify the increasing expression of these genes by real time PCR analysis.

3.3. Real-time PCR confirms the microarray results

Several caspase genes were found in the microarray profile. To determine whether caspases are involved in cRGD induced cell death, and to further validate the microarray results, we used quantitative real-time PCR to examine the effect of cRGD on caspase genes. RNA samples from each time point

Table 3
Time-course caspase gene expression measured by real-time Q-PCR experiments

	15 min	30 min	1 h	2 h	3 h	4 h	5 h	6 h	7 h
CASP 4	0.97 ± 0.05	0.69 ± 0.1	1.87 ± 0.18	0.79 ± 0.12	1.23 ± 0	2.22 ± 0.11	1.32 ± 0	1.07 ± 0	1.57 ± 0.08
CASP 6	1.15 ± 0.11	0.76 ± 0.07	1.23 ± 0	0.87 ± 0	1.00 ± 0.1	1.42 ± 0.14	1.23 ± 0.12	0.93 ± 0	1.37 ± 0.07
CASP 7	1.07 ± 0	0.79 ± 0.12	1.11 ± 0.05	0.79 ± 0.04	1.52 ± 0	1.01 ± 0.2	1.04 ± 0.05	0.93 ± 0	1.15 ± 0.11
CASP 9	1.04 ± 0.05	0.87 ± 0.09	1.28 ± 0.06	0.62 ± 0.06	1.32 ± 0	1.68 ± 0.08	1.07 ± 0	1.11 ± 0.05	1.63 ± 0.16
	8 h	9 h	10 h	12 h	24 h	36 h	48 h	60 h	72 h
CASP 4	1.19 ± 0.06	1.23 ± 0.12	0.84 ± 0.04	4.61 ± 0.45	2.3 ± 0	0.73 ± 0.04	1.07 ± 0	0.45 ± 0.02	1.07 ± 0.11
CASP 6	1.32 ± 0	1.46 ± 0.07	1.19 ± 0.06	2.22 ± 0.11	1.19 ± 0.06	0.68 ± 0.03	1.19 ± 0.06	0.56 ± 0.08	1.15 ± 0
CASP 7	0.87 ± 0.09	1.00 ± 0.1	1.07 ± 0	2.46 ± 0	2.55 ± 0.12	0.93 ± 0	1.46 ± 0.07	0.45 ± 0.02	0.97 ± 0.05
CASP 9	1.57 ± 0.08	1.68 ± 0.08	1.47 ± 0.22	1.75 ± 0.17	1.15 ± 0.11	1.32 ± 0	1.75 ± 0.17	1.00 ± 0.1	1.37 ± 0.07

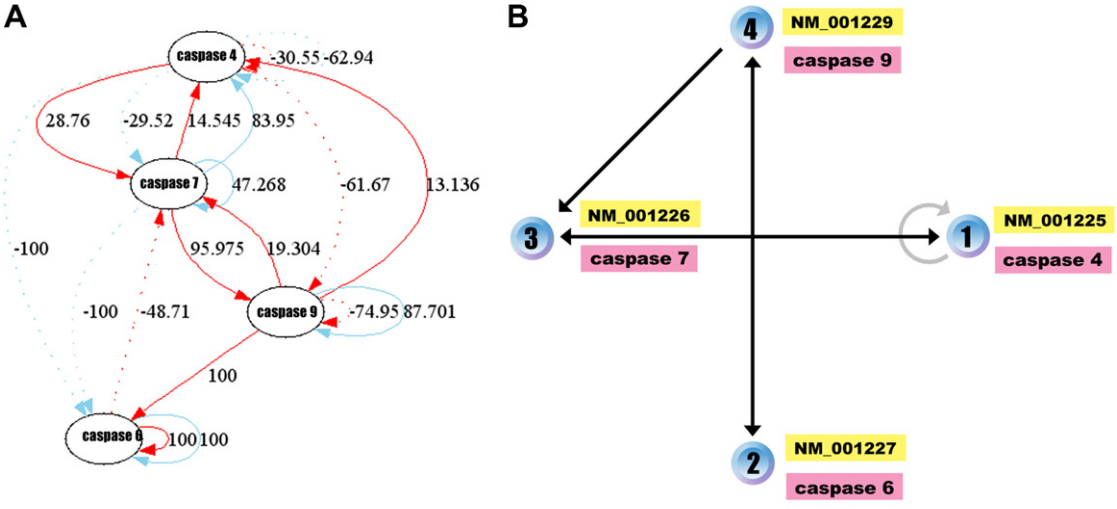

Fig. 4. Gene network construction. Two plausible gene regulatory networks were reconstructed by (A) BSIP and (B) GeneNetwork. They share similar gene regulation topology.

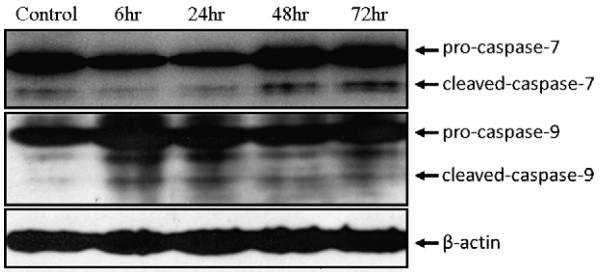

Fig. 5. Western blot analysis of controlled and cRGD-treated MCF-7 cells. The proteins extracted from MCF-7 cells, with control and in 6, 24, 48, and 72 h after cRGD treatment, were separated by one-dimensional electrophoresis (1DE), and then transferred onto PVDF membrane, respectively. The Western blots were performed for caspase-7 and caspase-9, respectively. Caspase-7 and caspase-9 were cleaved into active forms in MCF-7 cells after cRGD treatment.

were reverse-transcribed into cDNA and then quantitative PCR was performed as described in Section 2. Values for each gene were normalized to values obtained for β-actin and then a ratio of treated to control was calculated. The statistical analysis using EDGE, caspase-4, -6, -7, and, -9 exhibited significant deferential expressions within time intervals ($P < 0.05$). Table 3 shows the averages of three separate experiments with the standard deviations.

3.4. Reconstruction of caspase-involved gene regulatory network

As more high-throughput time-series measurements become available, various reverse engineering schemes have been developed to reconstruct the functional interaction structure from given time-series expression profiles [18,19]. The time-series expression levels of the selected candidate genes, caspase-4, -6, -7, and -9, were used to build up a potential gene interaction network. The inferred novel putative response pathway is shown in Fig. 4. Two software tools, GeneNetwork and BSIP, revealed a comparable signaling pathway. Both results indicate that the activation of caspase-9 will stimulate activation of caspase-7 and caspase-6, and capase-4 is aroused by activated capase-7. There are some positive feedback loops designated in Fig. 4B: caspase-9 and caspase-6, caspased-7 and caspase-4, and auto-activation of caspase-4.

3.5. Modulation of caspases in protein level

To investigate the modulation of caspases in protein level, we performed western blot analysis for caspase-7 and caspase-9. The proteins extracted from MCF-7 cells in control and at 6, 24, 48 and 72 h after cRGD treatment were separated by one dimensional electrophoresis, and then transferred onto PVDF membrane, respectively. Caspase-7 and caspase-9 in MCF-7 cells were cleaved into active forms after cRGD treatment, as shown in Fig. 5. Our results showed that caspase-7, as well as caspase-9, were up-regulated both in the level of transcript and protein for cRGD-treated MCF-7 cells. This indicates that the cell death caused by cRGD may be triggered through activation of caspase-7 and caspase-9.

4. Discussion

Synthetic peptides containing the RGD motif have been used extensively as inhibitors of integrin–ligand interactions [5]. By docking simulation, the cyclic RGD we designed shows a reliable binding affinity to integrin heterodimeric interface. It indicates that cRGD might be a potent drug for good binding affinity to tumor cells membrane. The microarray study of cRGD in MCF-7 provided the first clue of which genes are modulated. To our knowledge, the induction of caspases genes family in MCF-7 by cRGD is somewhat surprising and has not yet been reported before. Previously we found that cRGD induced a typical apoptosis in MCF-7 human breast carcinoma cancer cells [11]. Here, we continued our investigation on cRGD-induced apoptosis in MCF-7 cell line. The breast cancer cell line MCF-7 was chosen because of the lack of functional caspase-3 protein in this cell line. According to the typical RGD-induced apoptosis, caspase-3 is a key molecule regulating the signaling [5]. It would be important and interesting if we conduct a newly found caspase-3-independent apoptotic signaling pathway *via* integrin stimulation.

Our previous report [11] shows MCF-7 suffered apoptosis after the treatment of our designed cyclic Tpa-RGDWPC (cRGD). Additionally, there were several integrin-mediated proteins that were down-regulated in protein differential expression profile. By docking simulation, we found that cRGD can be docked in the integrin active site. These suggest that cRGD may mimic the RGD-binding motif of integrin-binding ligands to bind to integrin. However, this binding could not induce the signal pathway involved in cell growth and proliferation. Instead, cytocrhome *c* was released from mitochondrial intermembrane space and activated caspase-9 [20]. From cDNA microarray data and real-time Q-PCR analysis, several caspase genes were activated sequentially after the treatment of cRGD. And then the reconstruction of caspase gene network is conducted by time series data. In the network, caspase-9, located at the upstream, activates downstream effector caspase-7. The activation of caspase-9 is believed to be a well-defined outcome of the release of mitochondrial cytochrome *c* into the cytoplasm and its subsequent association with the Apaf-1 protein. The assembly of cytochrome *c*, Apaf-1 and procaspase-9, called apoptosome, triggers the activation of caspase-9 [21]. Subsequently, caspase-7 is directly activated by the Apaf-1-caspase-9 apoptosome [22]. This indicates that the cell death caused by cRGD may be triggered through activation of caspase pathway. Our results provide a molecular explanation of cRGD treatment in breast cancer cells and set forth a constructive far-reaching impact in breast cancer therapy.

Acknowledgements: This work was supported by NTU Frontier and Innovative Research Projects (NTU-PFIR-95R0107) and National Science Council of Taiwan. We also thank Nancy Lin for manuscript proofreading.

References

[1] Gerschenson, L.E. and Rotello, R.J. (1992) Apoptosis: a different type of cell death. Faseb J. 6, 2450–2455.
[2] Thompson, C.B. (1995) Apoptosis in the pathogenesis and treatment of disease. Science 267, 1456–1462.
[3] Pignatelli, M., Cardillo, M.R., Hanby, A. and Stamp, G.W. (1992) Integrins and their accessory adhesion molecules in mammary carcinomas: loss of polarization in poorly differentiated tumors. Hum. Pathol. 23, 1159–1166.
[4] Werb, Z. (1997) ECM and cell surface proteolysis: regulating cellular ecology. Cell 91, 439–442.

[5] Buckley, C.D., Pilling, D., Henriquez, N.V., Parsonage, G., Threlfall, K., Scheel-Toellner, D., Simmons, D.L., Akbar, A.N., Lord, J.M. and Salmon, M. (1999) RGD peptides induce apoptosis by direct caspase-3 activation. Nature 397, 534–539.
[6] Frisch, S.M. and Francis, H. (1994) Disruption of epithelial cell–matrix interactions induces apoptosis. J. Cell Biol. 124, 619–626.
[7] Price, L.S. (1997) Morphological control of cell growth and viability. Bioessays 19, 941–943.
[8] Broxterman, H.J. and Hoekman, K. (1999) Direct activation of caspases by RGD-peptides may increase drug sensitivity of tumour cells. Drug Resist. Updat. 2, 139–141.
[9] Adderley, S.R. and Fitzgerald, D.J. (2000) Glycoprotein IIb/IIIa antagonists induce apoptosis in rat cardiomyocytes by caspase-3 activation. J. Biol. Chem. 275, 5760–5766.
[10] Castel, S., Pagan, R., Mitjans, F., Piulats, J., Goodman, S., Jonczyk, A., Huber, F., Vilaro, S. and Reina, M. (2001) RGD peptides and monoclonal antibodies, antagonists of alpha(v)-integrin, enter the cells by independent endocytic pathways. Lab. Invest. 81, 1615–1626.
[11] Juan, H.F., Wang, I.H., Huang, T.C., Li, J.J., Chen, S.T. and Huang, H.C. (2006) Proteomics analysis of a novel compound: cyclic RGD in breast carcinoma cell line MCF-7. Proteomics 6, 2991–3000.
[12] Mpamhanga, C.P., Chen, B., McLay, I.M., Ormsby, D.L. and Lindvall, M.K. (2005) Retrospective docking study of PDE4B ligands and an analysis of the behavior of selected scoring functions. J. Chem. Inf. Model 45, 1061–1074.
[13] Venkatachalam, C.M., Jiang, X., Oldfield, T. and Waldman, M. (2003) LigandFit: a novel method for the shape-directed rapid docking of ligands to protein active sites. J. Mol. Graph. Model. 21, 289–307.
[14] Krammer, A., Kirchhoff, P.D., Jiang, X., Venkatachalam, C.M. and Waldman, M. (2005) LigScore: a novel scoring function for predicting binding affinities. J. Mol. Graph. Model. 23, 395–407.
[15] Brooks, B.R., Bruccoleri, R.E., Olafson, B.D., States, D.J., Swaminathan, S. and Karplus, M. (1983) CHARMM: A program for macromolecular energy, minimization, and dynamics calculations. J. Comput. Chem. 4, 187–217.
[16] Leek, J.T., Monsen, E., Dabney, A.R. and Storey, J.D. (2006) EDGE: extraction and analysis of differential gene expression. Bioinformatics 22, 507–508.
[17] Wu, C.C., Huang, H.C., Juan, H.F. and Chen, S.T. (2004) GeneNetwork: an interactive tool for reconstruction of genetic networks using microarray data. Bioinformatics 20, 3691–3693.
[18] Bar-Joseph, Z. (2004) Analyzing time series gene expression data. Bioinformatics 20, 2493–2503.
[19] D'Haeseleer, P., Liang, S. and Somogyi, R. (2000) Genetic network inference: from co-expression clustering to reverse engineering. Bioinformatics 16, 707–726.
[20] Zhao, H., Ross, F.P. and Teitelbaum, S.L. (2005) Unoccupied {alpha}v{beta}3 integrin regulates osteoclast apoptosis by transmitting a positive death signaled. Mol. Endocrinol. 19, 771–780.
[21] Zou, H., Li, Y., Liu, X. and Wang, X. (1999) An APAF-1.cytochrome c multimeric complex is a functional apoptosome that activates procaspase-9. J. Biol. Chem. 274, 11549–11556.
[22] Twiddy, D., Cohen, G.M., Macfarlane, M. and Cain, K. (2006) Caspase-7 is directly activated by the approximately 700-kDa apoptosome complex and is released as a stable XIAP-caspase-7 approximately 200-kDa complex. J. Biol. Chem. 281, 3876–3888.
[23] DeLano, W.L. (2002) The PyMOL Molecular Graphics System, DeLano Scientific, San Carlos, CA, USA.